The Egyptian Journal of Hospital Medicine (July 2025) Vol. 100, Page 4266-4278

Impact of Moringa Olifera Organometallic Nanoparticles in Treatment of Murine Trichinellosis

Esraa El-Sayed Ahmed Mohamed [1]*, Samar Saad El-Deen El-Sayed Ibrahim [1], Reda M. Abdelhameed [2], Fatma Mohamad El-Lessy [1], Doaa Abdel-Fattah Ahmed Amer[1]

[1] Department of Medical Parasitology, Faculty of Medicine for Girls, Al-Azhar University, Cairo, Egypt

[2] Department of Applied Organic Chemistry, Chemical Industries Research Institute, National Research Centre, 33 EL Buhouth St., Dokki, Giza, 12622, Egypt

*** Corresponding author:** Esraa El-sayed Ahmed Mohamed, Mobile: 01002323198, Email: esraamostafaa941@gmail.com

ABSTRACT

Background: Trichinellosis, caused by *Trichinella spiralis*, is a significant foodborne zoonosis. While Mebendazole remains the standard treatment, its side effects and emerging resistance highlight the need for alternatives. *Moringa oleifera* has recently emerged as a promising, safer therapeutic option. **Aim of the work:** This study evaluated the therapeutic efficacy of *Moringa oleifera* compared to Mebendazole in experimental murine trichinellosis.

Material and Methods: A total of 180 Swiss albino male mice were divided into two equal groups (intestinal and muscular group), each one subdivided into nine subgroups (n=10), including controls and different treatment regimens (Mebendazole, *Moringa*, Ca-IMZ, and their combinations). Efficacy was evaluated using parasitological, histopathological, and biochemical assessments. **Results:** All treated subgroups demonstrated significant reductions in *Trichinella spiralis* burdens during both the intestinal and muscular phases, albeit with variable degrees of efficacy. The combined Mebendazole@Ca-IMZ and *Moringa* @ Ca-IMZ demonstrated the highest efficacy (91.64% reduction in adult worms; 80.29% reduction in encysted larvae), whereas the lowest effects were recorded with single treatments, particularly *Moringa* alone in the intestinal phase (38.68%) and Ca-IMZ alone in the muscular phase (32.28%). Histopathological examination revealed marked improvements in dual therapies than monotherapies. Treatment with Mebendazole -loaded (intestinal phase) and carrier nano-formulations (muscular phase) resulted most pronounced reductions of liver enzymes, urea and creatinine. Nano-formulated therapies, particularly Mebendazole@ Ca-IMZ and its combination with Moringa@ Ca-IMZ provided the most effective restoration of redox balance.

Conclusion: *Moringa oleifera* exhibits promising a therapeutic potential against *T. spiralis*, particularly when delivered via nanoparticles or in combination with Mebendazole@ Ca-IMZ, achieving variable degrees of efficacy.

Keywords: *Moringa oleifera*; *Trichinella spiralis;* Mebendazole, nanoparticles.

INTRODUCTION

Trichinellosis is a globally distributed food-borne parasitic disease caused by the ingestion of raw or undercooked meat containing the larvae of *Trichinella* nematodes mainly *Trichinella* spiralis [1]. The parasite can infect more than 150 animal species, including humans, leading to a range of clinical manifestations in both animal and human hosts. According to the World Health Organization (WHO), the prevalence of trichinellosis in Egypt is estimated as approximately 10%. Epidemiological evidence indicates that both domestic and wild animals contribute to the transmission cycle in the country [2].

The treatment of trichinellosis poses several challenges. Antiparasitic therapy is most effective when administered during the early intestinal phase, ideally within the first week post-infection, before the release of newborn larvae. However, once the larvae become encapsulated within muscle tissue, conventional treatment becomes largely ineffective, as antiparasitic agents cannot adequately penetrate the fibrous capsules that enclose the encysted larvae deep within the tissues. Larvae can persist within muscle nurse cells for prolonged periods, up to 40 years in humans and more than 20 years in other host species [3]. Benzimidazole derivatives (e.g., Mebendazole) are among the conventional treatments for trichinellosis; however, they are associated with several adverse effects and are contraindicated during pregnancy and in children less than three years of age. Additionally, the emergence of Mebendazole resistance has been reported. Moreover, Mebendazole has limited efficacy against encapsulated larvae and suffers from low bioavailability [4]. In recent years, nanomaterials have emerged as promising delivery systems in the medical field, providing an innovative strategy to enhance the bioavailability of therapeutic agents and bioactive compounds. In medicine, organometallic compounds are increasingly recognized for their potential to enhance the therapeutic efficacy of herbal bioactive substances by improving their solubility, stability, and targeted delivery within the body [5]. *Moringa oleifera*, often called the "miracle tree" is a plant with a long history of medicinal use in traditional and folk medicine. Its various parts, including leaves, seeds and roots are employed to treat a wide array of ailments [6]. So, this study was to evaluate the efficacy of *Moringa oleifera* compared to Mebendazole in treating experimental murine trichinellosis, using parasitological, histopathological and biochemical assessments.

MATERIAL AND METHODS

The experimental work (Diagram 1) was carried out at the National Institutes of Health (NIH), Giza, Egypt, in collaboration with the Medical Parasitology Department, Faculty of Medicine for Girls, Al-Azhar University, Cairo, Egypt.

Received: 30/04/2025
Accepted: 30/06/2025

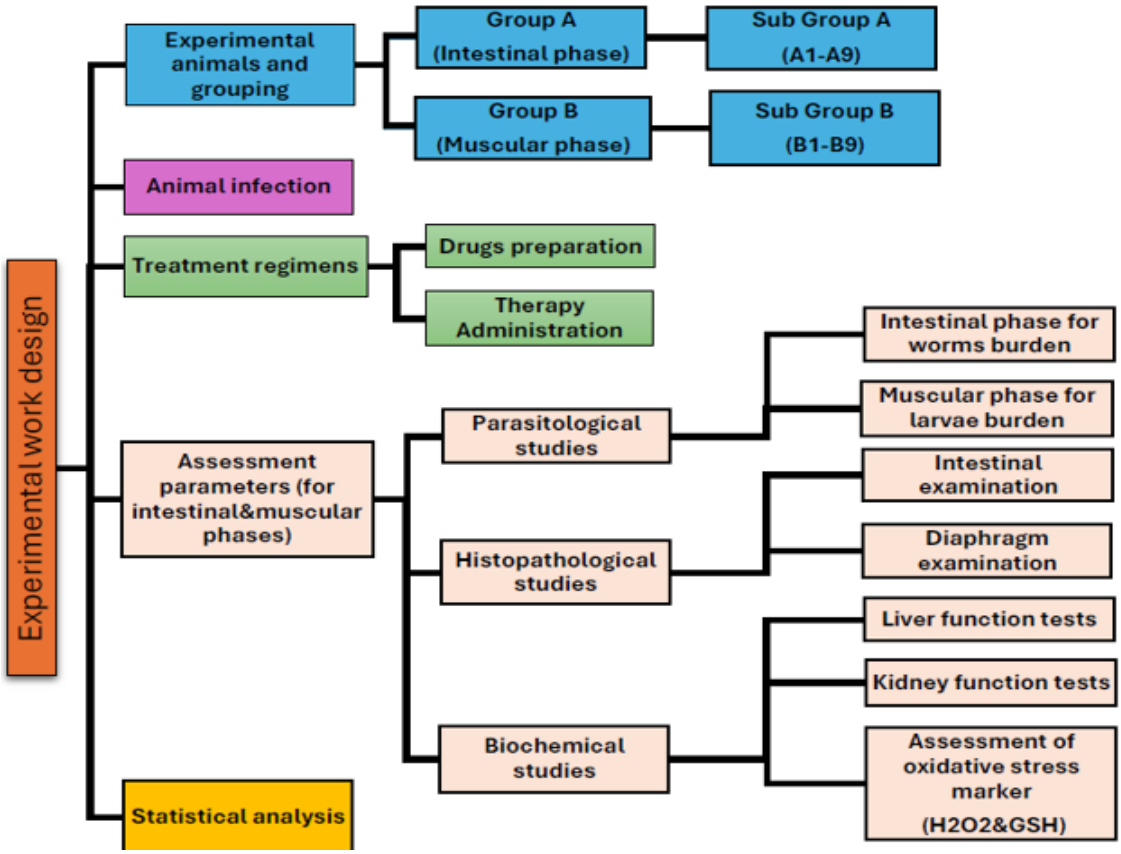

Diagram 1 The experimental work design.

Experimental animals and grouping

The present study was conducted on 180 laboratory-bred male Swiss albino mice, weighing 20–25 g and aged 4–6 weeks. They were pathogen-free and housed at suitable conditions according to NIH laboratory standards.

The mice were divided into two equal groups (90 mice each); Group A represented the intestinal phase of the parasite, while Group B represented the muscular phase. Each main group was subdivided into 9 subgroups, consisting of 10 mice each (Diagram 2).

Animal infection

Trichinella spiralis (*T. spiralis*) strain, originally obtained from infected pigs, was maintained at the Theodor Bilharz Research Institute (TBRI) through serial passage in Swiss albino mice. Infected mice were anesthetized, sacrificed and their diaphragms were incubated at 37 °C in a pepsin-HCl solution for 2 hours. The digest was then sieved, washed with saline, and sedimented to recover the larvae. Mice were starved for 12 hours prior to infection, then orally inoculated with approximately 200 living motile larvae using a tuberculin syringe.

Treatment regimens

Drugs preparation

a. **Mebendazole** tablets (100 mg; Vermox, Janssen, Egypt) were crushed and dissolved in distilled water to prepare the required dosage.

b. ***Moringa oleifera*** **Leaves Ethanolic Extract:** Fresh *Moringa* leaves were washed with distilled water, shade-dried at room temperature, and ground into a fine powder. One kilogram of powder was extracted with 1000 mL of absolute ethanol (99.8%) for 48 h and filtered twice through 2 µm filter paper. This extraction–filtration process was repeated three times. The pooled extract was stored in an airtight brown bottle at 4 °C, and ethanol was completely evaporated to obtain the alcohol-free dry product.

c. Synthesis of Ca-Imidazole (Ca-IMZ): Ca-IMZ was synthesized via a solvent-assisted stirring method in dimethylformamide (DMF). Imidazole (10.86 mg) was dissolved in 3 mL DMF, and calcium acetate dihydrate [$Ca(OAc)_2 \cdot 2H_2O$] (35.12 mg) was dissolved separately in 2 mL DMF. The calcium solution was added dropwise to the imidazole solution under continuous stirring for 30 min. The precipitate obtained was collected by centrifugation at 8000 rpm for 20 min and purified by washing with 15 mL DMF three times daily for three consecutive days, followed by the same procedure with 15 mL methanol. The dried Ca-IMZ product was characterized using X-ray diffraction (XRD), Fourier-transform infrared spectroscopy (FTIR), and scanning electron microscopy (SEM).

d. Mebendazole and *Moringa* leaves loading Prior to drug loading, Ca-IMZ was activated under vacuum at 25 °C for 12 h. For the loading process, 5 mg of Ca-IMZ was immersed in 1 mL of ethanol

containing either mebendazole (2 mg mL^{-1}) or *Moringa* leaves extract for varying durations (5–240 min). The suspensions were centrifuged at 8000 rpm for 20 min, and the resulting drug-loaded solids were collected, air-dried, and characterized using XRD, FTIR, and SEM. The supernatants were analyzed by UV–Vis spectroscopy, and standard calibration curves in ethanol were used to determine the concentration of unabsorbed drug or extract.

e. In vitro release of free Mebendazole and *Moringa* leaves extract:

Release studies were performed in PBS at pH 5.5 and 7.4 using the dialysis bag method. Free Mebendazole and *Moringa*, equivalent to the content in 50 mg of *Moringa* @Ca-IMZ, were dissolved in 1 mL PBS (sonication-assisted) and placed in dialysis bags. The bags were immersed in 5 mL PBS and incubated at 37 °C with shaking (200 rpm). At predetermined intervals, 200 µL aliquots were withdrawn and replaced with fresh PBS to maintain sink conditions. The concentrations and cumulative release percentages of Mebendazole and *Moringa* were determined using standard calibration curves prepared in PBS at both pH values.

Therapy Administration

Therapeutic interventions commenced on day 1 post-infection for the intestinal phase and on day 14 post-infection for the muscular phase [7]. All treatments were administered orally according to the dosages outlined in (Diagram 2).

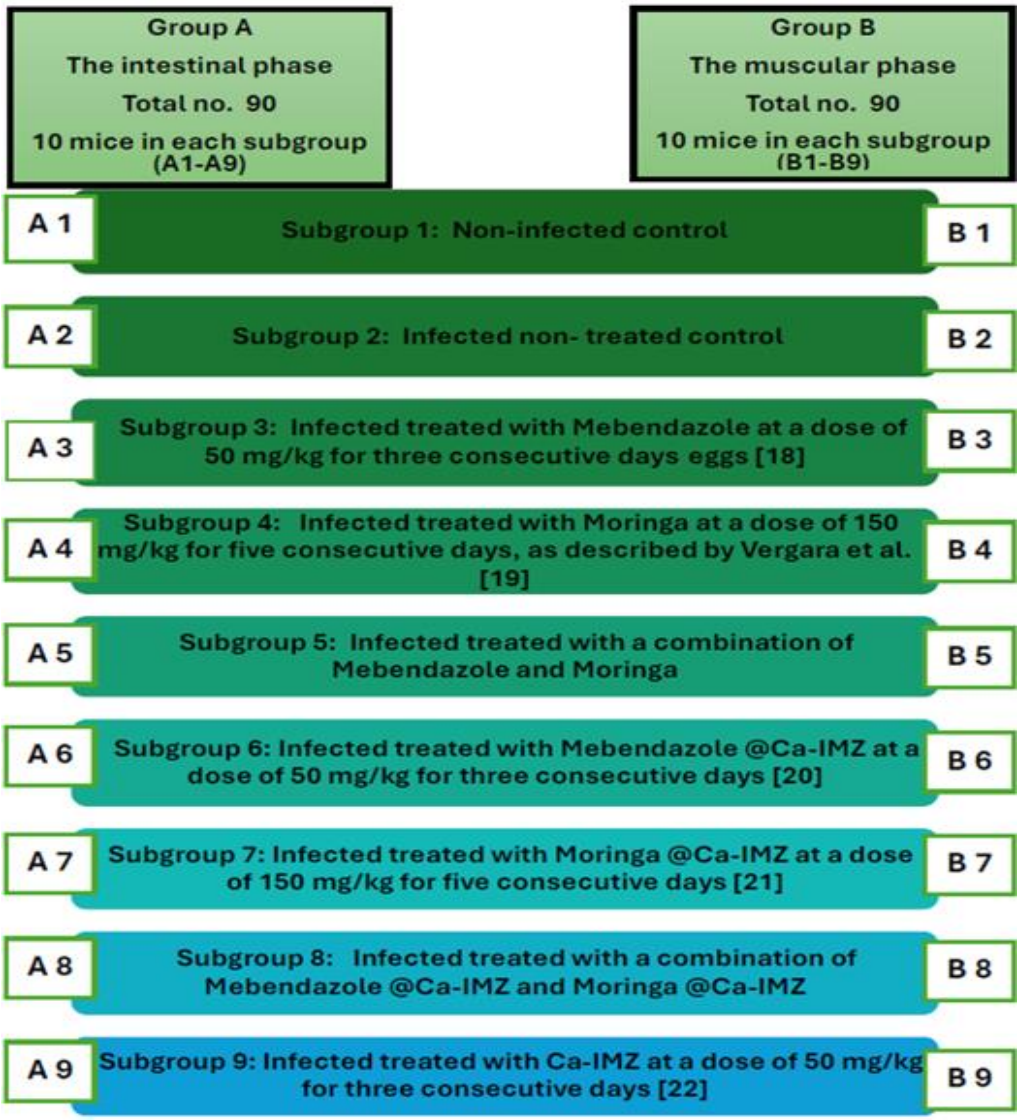

Diagram 2: Animal groups, subgroups and drugs doses.

Assessment parameters

Mice were sacrificed under anesthesia on day 6 post-infection for the intestinal phase and on day 36 post-infection for the muscular phase. Parasitological, histopathological and biochemical assessments were conducted for both phases.

Parasitological studies

Intestinal phase: The small intestines were excised and dissected longitudinally to collect the intestinal fluid, which was centrifuged and examined under a dissecting microscope to identify and count the adult worms per milliliter. **Muscular phase:** Diaphragm tissues were isolated, weighed, minced into small portions and then digested and centrifuged. Larvae were assessed microscopically from the resulting sediment and expressed per gram of tissue.

Histopathological studies: The excised small intestine (from the intestinal phase) and diaphragm specimens (from the muscular phase) were collected, fixed in 10% formol-saline, paraffin-embedded, sectioned at 4 µm and stained with Hematoxylin & Eosin (H&E) for microscopic examination.

Biochemical studies

Serum preparation: Blood was collected from the abdominal aorta during both the intestinal and muscular phases into a serum clot activator tube, centrifuged at 4000 g for 10 minutes at 4 °C to obtain serum which stored at −80 °C.

Liver function assessment: The activities of Alanine Aminotransferase (ALT) and Aspartate aminotransferase (AST) were measured according to the method of **Reitman and Frankel** [8], using commercial diagnostic kits (Biomaghreb, Tunisia; Randox, United Kingdom). **Kidney function tests:** According to **Patton and Crouch** [9], urea and creatinine were estimated, using assay kit.

Assessment of Oxidative Stress Markers in Tissue Homogenates: One gram of intestinal tissue (intestinal phase) and 0.5 grams of muscular tissue (muscular phase) were separately homogenized in 10 mL of phosphate-buffered saline (PBS) using an automated homogenizer. The resulting homogenates were filtered through filter paper and used for the assessment of oxidative stress markers; hydrogen peroxide (H_2O_2) and glutathione (GSH), using commercially available assay kits (Biodiagnostics, Egypt). All results were expressed as units per milliliter (U/mL) of tissue homogenate.

Ethical considerations

The experimental protocol was reviewed and approved by the Research Ethics Committee of the Faculty of Medicine for Girls, Al-Azhar University, Cairo, Egypt. All animal procedures were conducted in compliance with the institutional guidelines for the care and use of laboratory animals and adhered to the National Institutes of Health (NIH) Guide for the Care and Use of Laboratory Animals. Every effort was made to minimize animal suffering and to use the minimum number of animals required to achieve the scientific validity. This work has been carried out in accordance with the ethical principles for animal experimentation and international standards for research integrity according to Helsinki declaration.

Statistical analysis

Statistical analysis was performed using SPSS version 27 (IBM©, Chicago, IL, USA). Normality of data distribution was assessed using the Shapiro-Wilk test and histograms. Parametric quantitative data were expressed as mean ± standard deviation (SD) and analyzed using one-way ANOVA followed by Tukey's post hoc test. A two-tailed p-value < 0.05 was considered statistically significant.

RESULTS

Results of loading Mebendazole and *Moringa* leaves

a. Characterization of Ca-IMZ

Ca-IMZ was successfully synthesized via a stirring method and purified through repeated washing. XRD analysis revealed strong diffraction peaks at 2θ values of 6.8°, 9.7°, 11.4°, 13.7°, and 15.3°, consistent with the simulated Ca-IMZ pattern, confirming crystalline structure formation. FTIR spectra further verified coordination between Ca^{2+} ions and the IMZ linker, as evidenced by the disappearance of the free –COOH peak (~1700 cm^{-1}) and the emergence of characteristic COO^- vibrations (~1580 and ~1400 cm^{-1}). The retention of the C-N stretching band (1320–1350 cm^{-1}) indicated preservation of amino groups within the framework. SEM micrographs showed nanoscale particles (40–120 nm) with a tendency to agglomerate; supporting the material's suitability as a drug carrier. Drug loading studies demonstrated rapid adsorption of Mebendazole and *Moringa* within the first 60 min, with equilibrium reached at ~90 min. The maximum loading capacities were approximately 230 mg g^{-1} for Mebendazole and 280 mg g^{-1} for *Moringa*. The initial fast uptake was attributed to abundant active sites and strong drug–framework interactions, while subsequent stabilization reflected saturation of binding sites. These findings confirm that Ca-IMZ exhibits high drug-loading efficiency and strong potential as a Nano carrier for therapeutic applications.

b. Mechanism of Loading:

The successful incorporation of Mebendazole and *Moringa* extract into Ca-IMZ is attributed to multiple non-covalent interactions within the porous framework. Hydrogen bonding between NH groups of Ca-IMZ and hydroxyl/triazole moieties of Mebendazole and *Moringa* played a dominant role, while π–π stacking between aromatic rings of the linker and the drug molecules further stabilized the adsorption. Weak coordination between nitrogen atoms in the triazole ring and Ca^{2+} centers, together with van der Waals and hydrophobic interactions within the pores, enhanced binding affinity. These synergistic interactions indicate that Mebendazole and *Moringa* are not simply physisorbed on the surface but are effectively dispersed within the Ca-IMZ framework, consistent with PXRD and FTIR results (Fig. 1, a b).

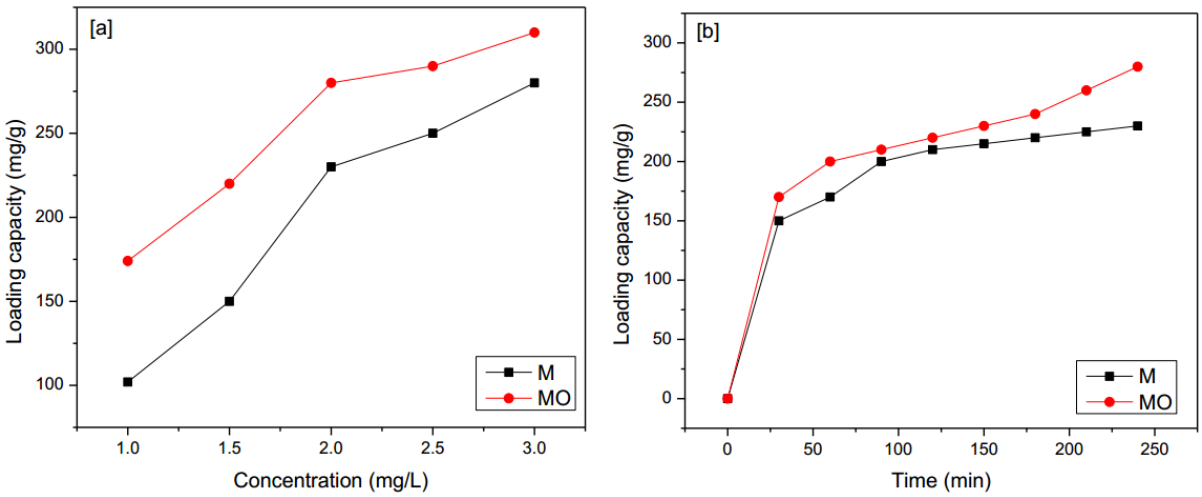

Fig.1: (a) Loading capacity of Ca-IMZ according to (Mebendazole (M) and *Moringa* (MO) concentration in ethanol solvent (240 min). (b) Drug adsorption efficiency of Ca-IMZ at Mebendazole (M) and *Moringa* (MO) concentration of 2 mg mL−1 in ethanol solvent.

c. Mebendazole and *Moringa* extract release

The release behavior of Mebendazole@Ca-IMZ and *Moringa* @Ca-IMZ was evaluated under physiological (pH 7.4) and acidic (pH 5.5) conditions. At pH 7.4, Mebendazole and *Moringa* exhibited a gradual release, reaching ~15% and ~24% after 2 h, and increasing to ~35% and ~55% after 48 h, respectively. In contrast, at pH 5.5, the release was significantly faster, with ~25% Mebendazole and ~35% *Moringa* released within the first hour, and cumulative release reaching ~73% and ~99% at 48 h. After 24 h, release at pH 7.4 was ~34% Mebendazole and ~54% *Moringa*, compared with ~69% Mebendazole and ~97% *Moringa* at pH 5.5.

These findings confirm that the nano system provides controlled and sustained release of MBZ and MO, with pH-dependent behavior that favors faster drug release in acidic conditions. This contrasts with the rapid and nearly complete release of free Mebendazole and *Moringa*, highlighting the potential of Mebendazole @Ca-IMZ and *Moringa*@Ca-IMZ as an efficient drug delivery platform for prolonged therapeutic action (Fig. 2).

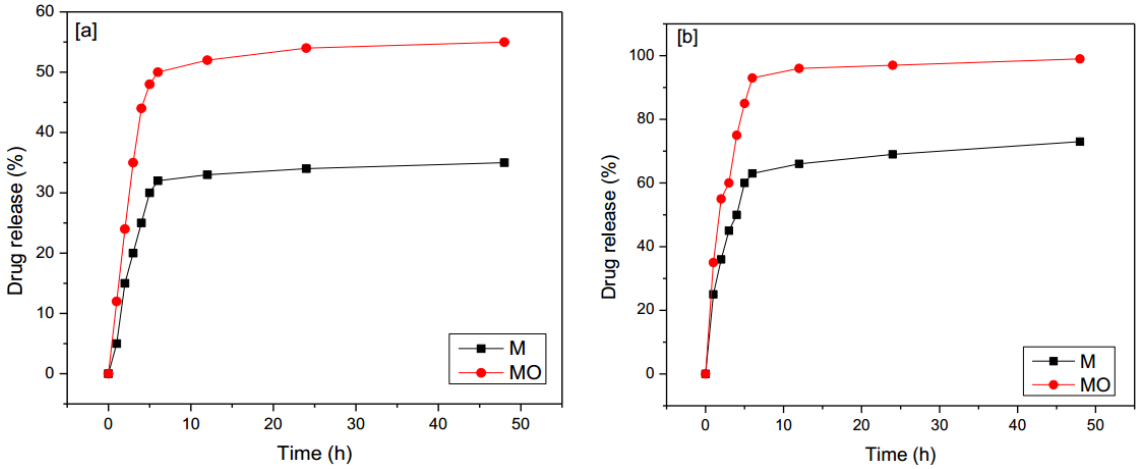

Fig. 2: The release of Mebendazole (M) and *Moringa* (MO) from Mebendazole@Ca-IMZ and *Moringa*@Ca-IMZ over time in PBS (a) pH 7.4 and (b)pH 5.5

Parasitological study results

Parasitological intestinal phase results

At day 6 post-infection, all treated intestinal phase subgroups (A3–A9) demonstrated a significant reduction in adult worm counts compared with the infected untreated control (A2). The highest reduction was observed in the subgroup treated with the combined Mebendazole@ Ca-IMZ and *Moringa* Ca-IMZ (A8; 91.64%), followed by the subgroup receiving the combination of Mebendazole and *Moringa* (A5; 82.46%). The lowest reductions were recorded in mice treated with *Moringa* alone (A4; 38.68%), Mebendazole alone (A3; 45.76%), and Ca-MOF alone (A9; 47.39%). Moderate reductions were achieved with *Moringa*@Ca-MOF (A7; 74.68%) and Mebendazole@Ca-IMZ (A6; 65.85%) (Table 1).

Table (1): Intestinal phase mean counts and percentages of reduction of the adult *T. spiralis* worms

Varieties / Animal groups	Intestinal worm load		Reduction (%)	P-value
	One-Way ANOVA test			
	Mean ± SD	Range		
A1	----	----	---	---
A2	86.1 ± 6.67	74 - 95	---	<0.001*
A3	46.7 ± 2.83	43 - 51	45.76%	<0.001*
A4	52.8 ± 2.35	50 - 56	38.68%	<0.001*
A5	15.1 ± 1.29	13 - 17	82.46%	<0.001*
A6	29.4 ± 2.27	25 - 33	65.85%	<0.001*
A7	21.8 ± 2.86	19 - 27	74.68%	<0.001*
A8	7.2 ± 2.35	4 - 10	91.64%	<0.001*
A9	45.3 ± 18.72	18 - 70	47.39%	<0.001*

A1: Non-infected control, A2: Infected non-treated control, A3: Infected treated with Mebendazole, A4: Infected treated with *Moringa*, A5: Infected treated with a combination of Mebendazole and *Moringa*, A6: Infected treated with Mebendazole@Ca-IMZ, A7: Infected treated with *Moringa*@Ca-IMZ, A8: Infected treated with a combination of Mebendazole@Ca-IMZ and *Moringa*@Ca-IMZ, A9: Infected treated with Ca-IMZ; SD: standard deviation, ANOVA: analysis of variance, P-value: probability value, %: percent, *: Significant p-value.

Parasitological muscular phase results

At day 36 post-infection, all treated muscular phase subgroups (B3–B9) showed a significant reduction in the mean counts of encysted larvae compared with the infected untreated control (B2). The highest reduction was observed in mice treated with the combination of Mebendazole@ Ca-IMZ and *Moringa* @ Ca-IMZ (B8; 80.29%), followed by Mebendazole@Ca-IMZ (B6; 74.52%), and the combination of Mebendazole and *Moringa* (B5; 69.20%). Mice treated with Mebendazole alone (B3; 57.53%) and *Moringa* alone (B4; 36.35%) showed moderate reductions. In contrast, Ca-IMZ alone (B9; 32.28%) produced the lowest reduction percentage (Table 2).

Table (2): Muscular phase mean counts and percentages of reduction of the *T. spiralis* larvae

Varieties / Animal groups	Larval burden on muscle		Reduction (%)	P-value
	One-Way ANOVA test			
	Mean ± SD	Range		
B1	----	----	---	---
B2	88.3 ± 7.97	76 - 105	---	<0.001*
B3	37.5 ± 3.21	33 - 42	57.53%	<0.001*
B4	56.2 ± 3.71	50 - 60	36.35%	<0.001*
B5	27.2 ± 1.99	25 - 30	69.20%	<0.001*
B6	22.5 ± 2.95	17 - 27	74.52%	<0.001*
B7	38.3 ± 2.31	35 - 42	56.63%	<0.001*
B8	17.4 ± 2.12	14 - 20	80.29%	<0.001*
B9	59.8 ± 5.27	51 - 68	32.28%	<0.001*

B1: Non-infected control, B2: Infected non-treated control, B3: Infected treated with Mebendazole, B4: Infected treated with *Moringa,* B5: Infected treated with a combination of Mebendazole and *Moringa,* B6: Infected treated with Mebendazole@Ca-IMZ, B7: Infected treated with *Moringa*@Ca-IMZ, B8: Infected treated with a combination of Mebendazole@Ca-IMZ and *Moringa*@Ca-IMZ, B9: Infected treated with Ca-IMZ; SD: standard deviation, ANOVA: analysis of variance, P-value: probability value, %: percent, *: Significant p-value.

Histopathological results

Histopathological intestinal phase results

The non-infected control group (A1) exhibited normal intestinal villi architecture. In contrast, the infected untreated control group (A2) showed marked villous length variabilities; cut sections of *T. spiralis* adults, and moderate inflammatory cell infiltration. All infected treated groups (A3–A10) displayed varying degrees of villous regeneration and recovery, accompanied by mild to minimal inflammatory infiltration. However, groups treated with *Moringa oleifera* alone (A4) or *Moringa*@ Ca-IMZ (A7) still harbored cut sections of *T. spiralis* adults. Notably, dual therapies; Mebendazole plus *Moringa* (A5) and Mebendazole@ Ca-IMZ plus *Moringa*@ Ca-IMZ (A8) achieved more pronounced villous restoration compared to monotherapies, with only minimal inflammatory cell infiltration (Fig. 3, A1–A9).

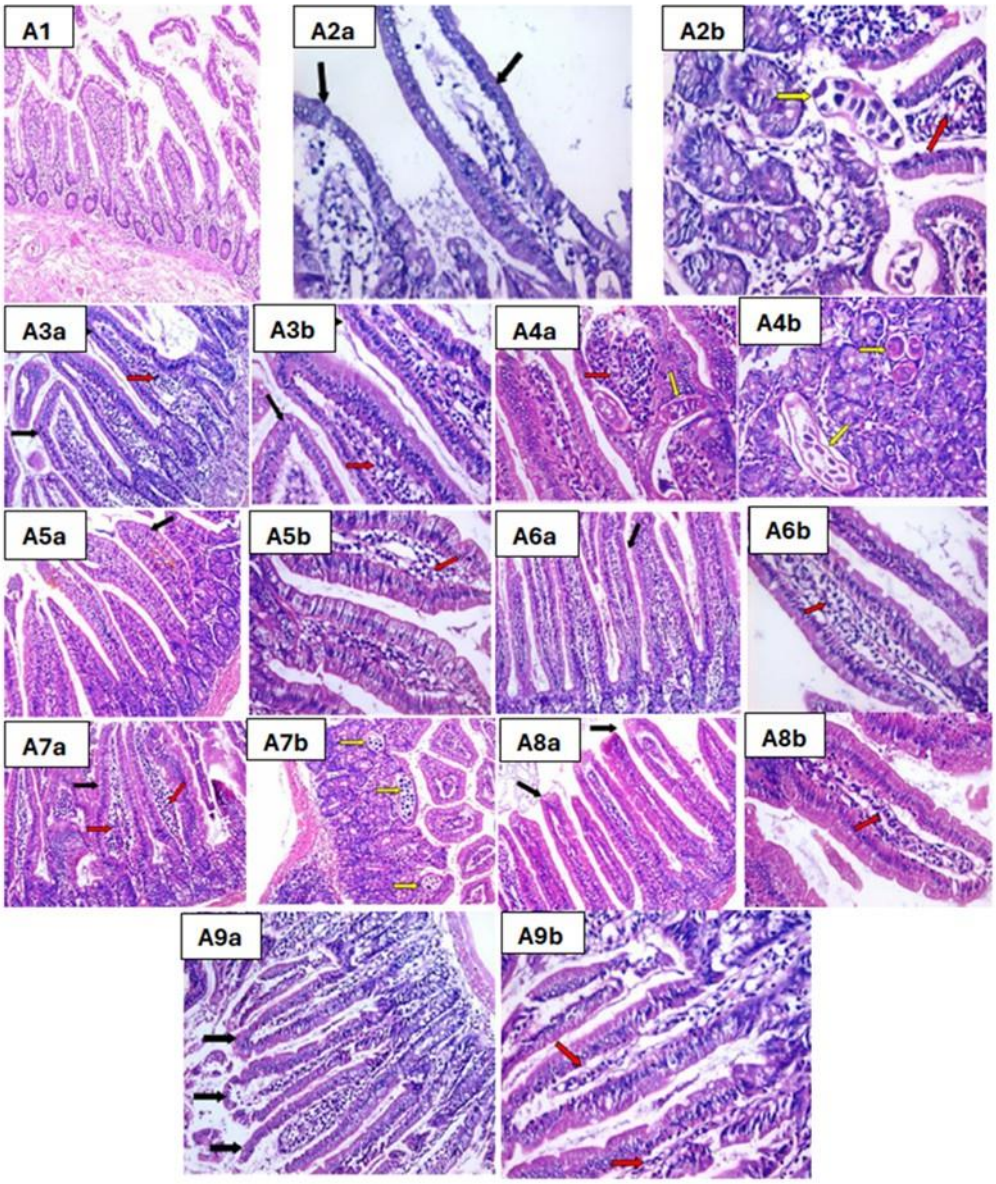

Fig. 3 Sections of small intestine stained with H&E from studied subgroups (A1–A9) on the day 6 PI; A1 (non-infected control) showed the normal villous architecture (100×). A2a&b (Infected non- treated control) showed variable villous length (black arrows), moderate inflammatory cell infiltration (red arrow), and cut sections in *T. spiralis* adults (yellow arrow) (200×). A3a & b (Infected treated with Mebendazole) showed moderate villous variability (black arrows), mild infiltration (red arrows), and absence of larvae (200×). A4a&b (Infected treated with *Moringa*) showed moderate infiltration (red arrow) and cut sections in adults (yellow arrows) (200×). A5a&b (Infected treated with a combination of Mebendazole and *Moringa*) showed regular villi (black arrow), minimal infiltration (red arrow) and no larvae (200×). A6a&b (Infected treated with Mebendazole@ Ca-IMZ) showed regular villi (black arrow), minimal infiltration (red arrow), and no detectable larvae (200×). A7a&b (Infected treated with *Moringa* Ca-IMZ) showed focally distorted villi (black arrow), moderate infiltration (red arrows) and cut sections in *T. spiralis* adults (yellow arrows) (200×). A8a&b (Infected treated with a combination of Mebendazole@Ca-IMZ and *Moringa*@ Ca-IMZ) showed regular villi (black arrow), minimal infiltration (red arrow), and no larvae. A9a&b (Infected treated with Ca-IMZ) showed regular villi (black arrows), mild infiltration (red arrows) and no larvae (200×).

Histopathological muscular phase results

Histopathological examination of the diaphragm muscles in the non-infected control group (B1) revealed normal muscle fiber architecture. In contrast, the infected untreated control group (B2) exhibited numerous encysted larvae with intact capsules, accompanied by moderate inflammatory cell infiltration. Infected mice treated with monotherapies; Mebendazole (B3), *Moringa* (B4), and Ca-IMZ (B9) still showed many encysted larvae and moderate inflammatory infiltrates surrounding the capsules. Conversely, dual-therapy subgroups, including Mebendazole plus *Moringa* (B5), Mebendazole@Ca-IMZ (B6), *Moringa*@Ca-IMZ (B7), and the combined Mebendazole@Ca-IMZ plus *Moringa*@Ca-IMZ (B8), displayed only a few cysts characterized by mild inflammatory infiltrates, marked larval degeneration, and destruction of cyst capsules (Fig. 4, B1–B9).”

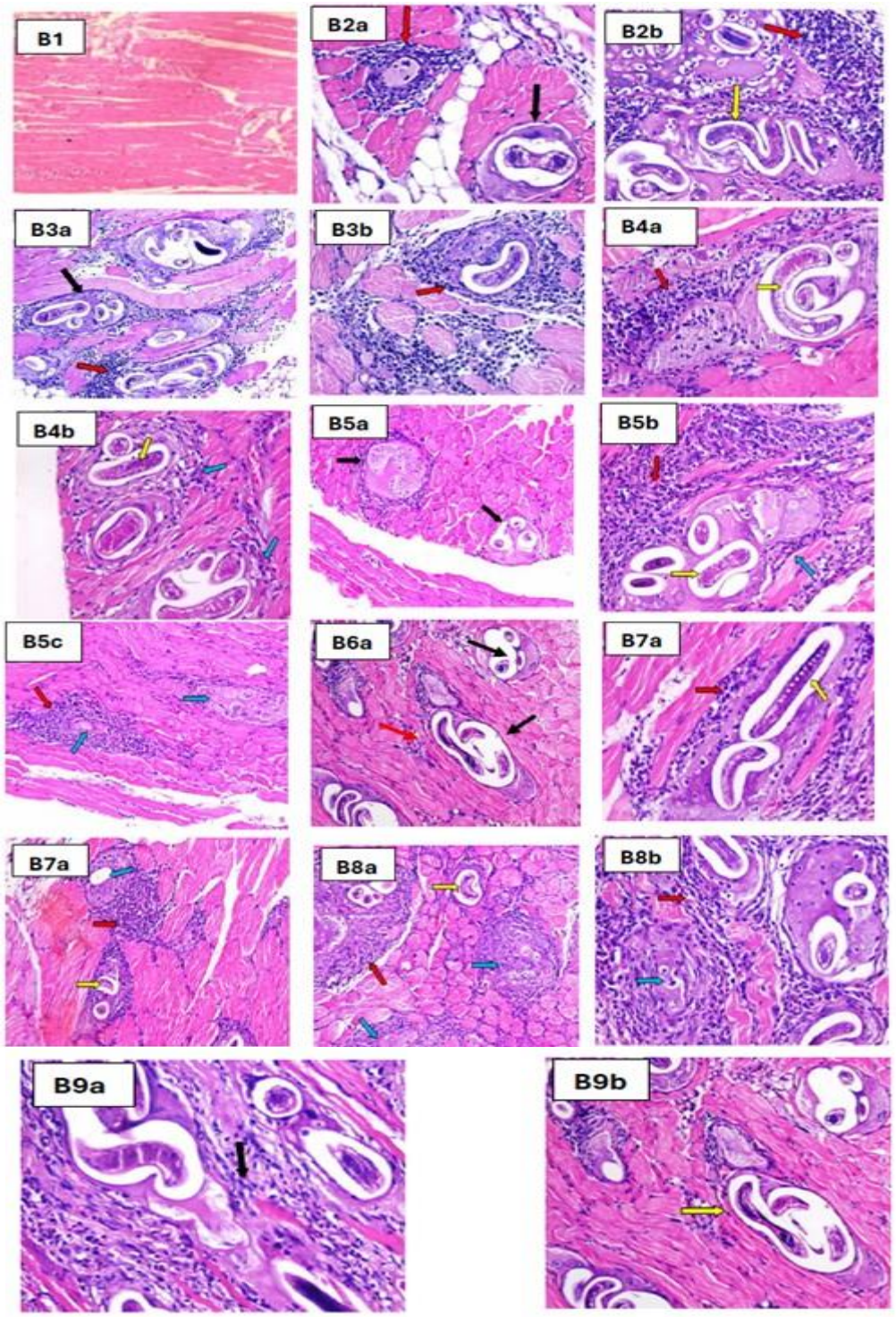

Fig. 4: Sections of diaphragm muscles stained with H&E from studied subgroups (B1-B9) on the day 36 post-infection; B1 (non-infected control) showed normal muscle architecture (100×). B2a&b (Infected non- treated control) showed numerous encysted larvae (yellow arrow) with intact capsules (black arrow), accompanied by moderate inflammatory cell infiltration (red arrows) (200×). B3a&b (Infected treated with Mebendazole) showed fewer encysted larvae with intact capsules (black arrow) and inflamed capsules (red arrows) (200×). B4a&b (Infected treated with *Moringa*) showed

many cysts with intact larvae (yellow arrows), focally degenerated capsules (blue arrows), with moderate inflammatory cell infiltration (red arrow) (200×). B5a&b (Infected treated with a combination of Mebendazole and *Moringa*) showed few cysts (black arrows) with intact larvae (yellow arrow), degenerated larvae and capsules (blue arrow) and moderate inflammatory infiltration (red arrow) (200×). B6a (Infected treated with Mebendazole@ Ca-IMZ) showed few cysts with degenerated capsules (black arrows) and moderate infiltration (red arrow). (200×). B7a&b (Infected treated with *Moring@* Ca-IMZ) showed few cysts with intact larvae (yellow arrows) and degenerated larvae and capsules (blue arrows), and focally mild infiltration (200×). B8a&b (Infected treated with a combination of Mebendazole@Ca-IMZ and *Moringa*@Ca-IMZ) showed few cysts with intact larvae (yellow arrow), focally degenerated larvae and capsules (blue arrows), and mild infiltration (red arrows) (200×).

Results of the Biochemical studies results:

Results of serum ALT and AST in both intestinal and muscular phases

Serum ALT and AST levels were significantly elevated ($p < 0.001$) in all infected subgroups during both the intestinal and muscular phases compared with the non-infected controls. The highest enzyme levels were observed in the infected untreated controls (A2: ALT 188.57 ± 1.04, AST 215.69 ± 1.45; B2: ALT 185.4 ± 2.27, AST 211.3 ± 3.08). In the intestinal phase, the greatest improvement was observed with Mebendazole@Ca-IMZ treatment (A6: ALT 99.58 ± 1.16, AST 113.54 ± 1.54) (Table 3). In the muscular phase, the most pronounced hepatoprotective effect was achieved with Ca-IMZ alone (B9: ALT 81.6 ± 3.03, AST 95.7 ± 0.93) (Tables 4).

Table (3): Mean and range of ALT and AST in intestinal phase

Varieties / Animal groups	ALT (u/ml)		P-value	AST (u/ml)		P-value
	One-Way ANOVA test			One-Way ANOVA test		
	Mean ± SD	Range		Mean ± SD	Range	
A1	39.28 ± 1.91	37.2 - 42.1		45.66 ± 1.8	43.3 - 47.7	
A2	188.57 ± 1.04	186.9 - 189.9	<**0.001***	215.69 ± 1.45	213.8 - 217.8	<**0.001***
A3	161.47 ± 1.54	158.9 - 164.1	<**0.001***	195.85 ± 1.22	193.6 - 197.4	<**0.001***
A4	141.25 ± 0.97	139.6 - 142.6	<**0.001***	154.36 ± 0.95	152.8 - 155.8	<**0.001***
A5	145.65 ± 0.81	144.4 - 146.7	<**0.001***	167.25 ± 1.23	165.3 - 168.6	<**0.001***
A6	99.58 ± 1.16	97.5 - 101.3	<**0.001***	113.54 ± 1.54	111.4 - 115.5	<**0.001***
A7	123.68 ± 2.22	119.8 - 125.9	<**0.001***	134.58 ± 1.08	133.3 - 136.5	<**0.001***
A8	112.69 ± 1.42	110.7 - 114.6	<**0.001***	122.36 ± 0.97	120.7 - 123.5	<**0.001***
A9	162.1 ± 0.65	161 - 163.2	<**0.001***	198.4 ± 1.62	196.4 - 200.7	<**0.001***

A1–A9: As defined in Table 1; ALT: alanine aminotransferase, AST: aspartate aminotransferase, U/ml: units per milliliter, SD: standard deviation, ANOVA: analysis of variance, P-value: probability value, *: Significant p-value.

Table (4): Mean and range of ALT and AST in muscular phase

Varieties / Animal groups	ALT (u/ml)		P-value	AST (u/ml)		P-value
	One-Way ANOVA test			One-Way ANOVA test		
	Mean ± SD	Range		Mean ± SD	Range	
B1	39.3 ± 2.03	37.3 - 42.9		45.7 ± 2.06	42.6 - 48.8	
B2	185.4 ± 2.27	182.5 - 188.5	<**0.001***	211.3 ± 3.08	208.1 - 216.2	<**0.001***
B3	158.4 ± 7.07	142.9 - 166.7	<**0.001***	191.5 ± 2.79	187.8 - 195.5	<**0.001***
B4	139.4 ± 2.8	135.7 - 142.9	<**0.001***	151.5 ± 1.68	148.9 - 153.7	<**0.001***
B5	141.02 ± 2.16	138.2 - 143.5	<**0.001***	159.7 ± 1.82	156.3 - 161.6	<**0.001***
B6	95.4 ± 1.64	92.9 - 97.7	<**0.001***	108.7 ± 2.54	104 - 112.5	<**0.001***
B7	121.05 ± 3.19	117.4 - 126.4	<**0.001***	130.6 ± 1.77	127.4 - 132.9	<**0.001***
B8	115.7 ± 2.22	112.7 - 118.8	<**0.001***	118.7 ± 1.96	115.9 - 121.8	<**0.001***
B9	81.6 ± 3.03	76.7 - 85.2	<**0.001***	95.7 ± 0.93	93.9 - 97.2	<**0.001***

B1–B9: As defined in Table 2; ALT: alanine aminotransferase, AST: aspartate aminotransferase, U/ml: units per milliliter, SD: standard deviation, ANOVA: analysis of variance, P-value: probability value, *: Significant p-value.

Results of serum urea and creatinine in both intestinal and muscular phases

Serum urea and creatinine levels were significantly elevated ($p < 0.001$) in all infected subgroups during both the intestinal and muscular phases compared with the non-infected controls, with the highest values recorded in the non-treated controls (A2, B2), indicating marked renal impairment. All treated groups showed significant reductions relative to the infected non-treated controls, though the extent of recovery varied. The greatest improvement was observed in subgroups treated with Mebendazole@ Ca-IMZ (A6) in intestinal phase, and infected treated with Ca-IMZ (B9) in muscular phase, where values approached normal levels (Tables 5&6).

Table (5): Mean and range of urea and creatinine in intestinal phase

Varieties / Animal groups	Urea (nmol/ml)		P-value	Creatinine (mg/dl)		P-value
	One-Way ANOVA test			One-Way ANOVA test		
	Mean ± SD	Range		Mean ± SD	Range	
A1	3.56 ± 0.44	2.8 - 4.4		2.99 ± 0.52	1.9 - 3.7	
A2	11.36 ± 1.09	10.2 - 13.8	<**0.001***	15.25 ± 0.95	14.2 - 16.7	<**0.001***
A3	8.65±0.63	7.8 - 9.7	<**0.001***	12.58 ± 0.82	11.4 - 13.6	<**0.001***
A4	7.25±1.46	5.3 - 9.6	<**0.001***	10.25 ± 0.87	8.9 - 11.4	<**0.001***
A5	8.01 ± 0.75	7.3 - 9.5	<**0.001***	11.25 ± 0.67	10.3 - 12.4	<**0.001***
A6	5.25±0.73	4 - 6.4	<**0.001***	7.25 ± 0.99	6.3 - 9.4	<**0.001***
A7	6.44±0.95	4.8 - 7.9	<**0.001***	10.36 ± 1.11	9.4 - 12.4	<**0.001***
A8	6.95±1.19	4.8 - 8.8	<**0.001***	8.25 ± 1.14	6.7 - 10.4	<**0.001***
A9	8.8 ±0.79	7.3 - 9.5	<**0.001***	12.6 ± 1.43	10.6 - 14.8	<**0.001***

A1–A9: As defined in Table 1; Urea: blood urea concentration, Creatinine: serum creatinine concentration, nmol/ml: nanomoles per milliliter, mg/dl: milligrams per deciliter, SD: standard deviation, ANOVA: analysis of variance, P-value: probability value, *: Significant p-value.

Table (6): Mean and range of urea & creatinine in muscular phase

Varieties / Animal groups	Urea (nmol/ml)		P-value	Creatinine (mg/dl)		P-value
	One-Way ANOVA test			One-Way ANOVA test		
	Mean ± SD	Range		Mean ± SD	Range	
B1	3.6 ± 0.77	2.4 - 4.7		3 ± 0.72	1.9 - 3.8	
B2	13.5 ± 0.89	12 - 15.1	<**0.001***	16.9 ± 1.15	14.8 - 18.3	<**0.001***
B3	9.5 ± 0.78	8.3 - 10.5	<**0.001***	13.6 ± 0.98	12.1 - 15.3	<**0.001***
B4	7.6 ± 0.88	6.3 - 8.9	<**0.001***	9.9 ± 1.18	7.4 - 11.2	<**0.001***
B5	8.1 ± 0.94	6.7 - 9.4	<**0.001***	13.6 ± 1.09	11.5 - 15.2	<**0.001***
B6	5.1 ± 0.85	3.7 - 6.7	<**0.001***	8 ± 1.24	6.5 - 9.5	<**0.001***
B7	6.1 ± 0.79	4.8 - 7.3	<**0.001***	11.1 ± 0.69	10.3 - 12.5	<**0.001***
B8	7 ± 0.58	5.8 - 7.8	<**0.001***	9 ± 0.87	7.3 - 9.8	<**0.001***
B9	4.6 ± 0.8	3.1 - 6.1	0.150	5.2 ± 1.12	3.5 - 7.2	<**0.001***

B1–B9: As defined in Table 2; Urea: blood urea concentration, Creatinine: serum creatinine concentration, nmol/ml: nanomoles per milliliter, mg/dl: milligrams per deciliter, SD: standard deviation, ANOVA: analysis of variance, P-value: probability value, *: Significant p-value.

Results of oxidative stress markers (H_2O_2 and GSH) in intestinal and muscular phases

Both intestinal and muscular phases of infection were characterized by pronounced oxidative stress, as evidenced by markedly elevated H_2O_2 levels and depleted GSH concentrations in the untreated groups (A2 and B2). All treatment regimens significantly attenuated oxidative damage to varying degrees, with groups A6 (H_2O_2: 43.7 ± 1.48, GSH: 3.58 ± 0.8) and A8 (H_2O_2: 35.4 ± 1.45, GSH: 3.11 ± 0.64) in the intestinal phase, together with B6 (H_2O_2: 41.6 ± 1.9, GSH: 3.5 ± 0.77) and B8 (H_2O_2: 36.1 ± 1.7, GSH: 3.1 ± 0.77) in the muscular phase, showing the most effective restoration of redox balance. By contrast, groups A9 and B9 retained persistently high H_2O_2 levels, with GSH recovery observed in the muscular phase (B9), indicating limited therapeutic efficacy. (Tables 7&8).

Table (7): The Mean and range of H_2O_2 & GSH in intestinal phase

Varieties / Animal groups	H_2O_2 (nmol/mg/protein)		P-value	GSH (nmol/mg/protein)		P-Value
	One-Way ANOVA test			One way ANOVA test		
	Mean ± SD	Range		Mean ± SD	Range	
A1	8.5 ± 0.84	7.4 - 9.8		4.91 ± 0.53	3.9 - 5.7	
A2	56.5 ± 0.8	55.4 - 57.8	**<0.001***	0.95 ± 0.24	0.6 - 1.3	**<0.001***
A3	16.4 ± 1.03	14.8 - 17.9	**<0.001***	1.55 ± 0.48	0.7 - 2.2	**<0.001***
A4	21.9 ± 1.38	19.5 - 23.7	**<0.001***	2.11 ± 0.58	1.3 - 3.3	**<0.001***
A5	20.4 ± 1.21	18.6 - 22.3	**<0.001***	1.95 ± 0.28	1.6 - 2.3	**<0.001***
A6	43.7 ± 1.48	42.2 - 45.8	**<0.001***	3.58 ± 0.8	2.6 - 5.2	**<0.001***
A7	33.7 ± 1.35	32.1 - 36.7	**<0.001***	2.51 ± 0.62	1.6 - 3.5	**<0.001***
A8	35.4 ± 1.45	33.1 - 37.3	**<0.001***	3.11 ± 0.64	2.3 - 4.5	**<0.001***
A9	75.8 ± 1.81	72.2 - 77.8	**<0.001***	1.7 ± 0.52	1.1 - 2.4	**<0.001***

A1–A9: As defined in Table 1; H_2O_2: hydrogen peroxide, GSH: reduced glutathione, nmol/mg/protein: nanomoles per milligram of protein, SD: standard deviation, ANOVA: analysis of variance, P-value: probability value, *: Significant p-value.

Table (8): Mean and range of H_2O_2 & GSH in muscular phase

Varieties / Animal groups	H_2O_2 (nmol/mg/protein)		P-value	GSH (nmol/mg/ protein)		P-value
	One-Way ANOVA test			One-Way ANOVA test		
	Mean ± SD	Range		Mean ± SD	Range	
B1	9.1 ± 0.71	8.4 - 10.1		4.9 ± 1	3.3 - 6.3	
B2	56.2 ± 2	52.8 - 59.3	**<0.001***	0.9 ± 0.43	0.1 - 1.4	**<0.001***
B3	16.9 ± 1.25	15.2 - 18.4	**<0.001***	1.7 ± 0.18	1.4 - 1.9	**<0.001***
B4	22.8 ± 1.83	19.5 - 24.7	**<0.001***	2.2 ± 0.79	1.4 - 3.4	**<0.001***
B5	20.2 ± 0.78	18.9 - 21.2	**<0.001***	2 ± 0.32	1.6 - 2.6	**<0.001***
B6	41.6 ± 1.9	39.4 - 45.6	**<0.001***	3.5 ± 0.77	2.1 - 4.2	**<0.001***
B7	34.4 ± 1.21	32.7 - 36.4	**<0.001***	2.6 ± 0.57	1.8 - 3.7	**<0.001***
B8	36.1 ± 1.7	33.2 - 38.9	**<0.001***	3.1 ± 0.77	2.1 - 4.5	**<0.001***
B9	75.7 ± 1.34	73.3 - 77.9	**<0.001***	3.8 ± 0.53	3.1 - 5	**0.008***

B1–B9: As defined in Table 2; H_2O_2: hydrogen peroxide, GSH: reduced glutathione, nmol/mg/protein: nanomoles per milligram of protein, SD: standard deviation, ANOVA: analysis of variance, P-value: probability value, *: Significant p-value.

DISCUSSION

Trichinellosis is a serious and globally prevalent parasitic disease. It provokes inflammatory reactions in the invaded tissues, which may become life-threatening if they spread to vital organs such as the lungs, heart, or central nervous system [10]. This study was designed to evaluate the effect of *Moringa oleifera* versus Mebendazole in managing experimental murine trichinellosis.

All treated subgroups showed significant reductions in *T. spiralis* burdens during both intestinal and muscular phases. The combined Mebendazole@Ca-IMZ and *Moringa*@Ca-IMZ demonstrated the highest efficacy (91.64% reduction in adult worms; 80.29% reduction in encysted larvae), whereas the lowest effects were recorded with single treatments, particularly *Moringa* alone in the intestinal phase (38.68%) and Ca-IMZ alone in the muscular phase (32.28%).

While no prior studies have specifically investigated the efficacy of *Moringa oleifera* against *T. spiralis*, its antiparasitic potential has been demonstrated against other parasites. **El-Sayed *et al.*** [11] reported a 30% reduction in *Cryptosporidium parvum* oocysts following treatment with *Moringa oleifera*. **Saad El-Din *et al.*** [12] confirmed its efficacy when used alone or in combination with praziquantel against *Schistosoma mansoni*. Moreover, **Abdel-Latif *et al.*** [13] demonstrated that *Moringa oleifera* enhanced intestinal immunity, achieving an 89.3% worm reduction in *Hymenolepis nana* infection.

Previous studies consistently confirmed the potential of nanoparticle-based formulations in enhancing anti-*Trichinella* efficacy. In the present study, calcium–nano-loaded Mebendazole and *Moringa oleifera* demonstrated superior therapeutic effects compared to their crude forms. This aligns with earlier reports highlighting the ability of calcium nanoparticles to enhance drug bioactivity [14] and augment the therapeutic potential of *Moringa oleifera* [15]. Likewise, **Abd-ELrahman *et al.*** [16] emphasized the efficiency of calcium nanoparticles as drug delivery systems,

improving the efficacy of both synthetic and natural agents in the treatment of *T. Spiralis*.

Mebendazole nano-formulations have been shown to enhance dissolution, pharmacokinetics, and bioavailability in the treatment of *T. spiralis* [17]. In line with this, mebendazole-loaded chitosan nanoparticles achieved over 96% larval reduction [18], while **El-Melegy *et al.*** [19] reported a 92.25% reduction using mebendazole-loaded silver nanoparticles, compared to less than 41% when either agent was used alone.

Regarding the histopathological findings of the small intestine, the infected untreated control group exhibited severe destruction of villous architecture, moderate inflammatory cell infiltration, and the presence of adult worms, consistent with previous reports by **Fadil *et al.*** [20] and **El-Wakil *et al.*** [21]. Administration of dual therapies resulted in marked improvement of these pathological alterations, demonstrating superior restorative effects compared to monotherapies, in agreement with **Hassan *et al.*** [21]. In contrast, groups treated with *Moringa oleifera* alone or *Moringa*@Ca-IMZ still harbored adult worms and showed moderate amelioration of intestinal lesions. These findings align with **El-Sayed *et al.*** [11], who reported that *Moringa* treatment led to partial improvement of intestinal pathology in *Cryptosporidium parvum* infection but was insufficient to achieve complete histological recovery.

In the muscular sections, the infected untreated control group exhibited numerous encysted larvae surrounded by moderate inflammatory infiltration, consistent with previous reports by **Fadil *et al.*** [20] and **El-Wakil *et al.*** [21]. In contrast, dual therapies resulted in the most pronounced reduction and destruction of larvae, followed by monotherapies, highlighting their superior efficacy, in agreement with **Hassan *et al.*** [4].

Serum liver enzymes, urea, and creatinine levels were significantly elevated in all infected subgroups during both the intestinal and muscular phases, reflecting marked hepatic and renal injury in agree with **Nasreldin *et al.*** [22]. Treatment with Mebendazole Mebendazole@Ca-IMZ (intestinal phase) and Ca-IMZ (muscular phase) produced the most pronounced reductions in these parameters. Similarly, several studies have reported that dual therapy or nanoparticle-based delivery systems effectively lower liver enzyme, urea, and creatinine elevations associated with *T. spiralis* infection [23, 24]. These findings suggest that such formulations not only reduce parasitic burden but also confer hepato-renal protective effects, underscoring their dual therapeutic potential.

During a *T. spiralis* infection, the host's eosinophils release hydrogen peroxide (H_2O_2) to help in destruction of larvae, but this process contributes to oxidative stress, which is characterized by increased H_2O_2 and decreased reduced glutathione (GSH) levels, leads to a state of oxidative stress, making the host more vulnerable to tissue damage. Antioxidant treatments, especially herbal compounds, restore GSH, enhance host defenses, and lower parasite burden [25, 26].

In the current study, Mebendazole alone produced moderate improvements in oxidative stress markers, whereas nano-formulated therapies, particularly MebendazoleCa-IMZ and its combination with *Moringa*@ Ca-IMZ achieved the most effective restoration of redox balance, nearly normalizing GSH levels and reducing H_2O_2 concentrations. In contrast, Ca-IMZ alone was largely ineffective, as indicated by persistently high H_2O_2 levels (A9 and B9) and GSH recovery in muscular phase only (B9).

Daré and Lautenschlager [27] reported that nanoparticles exert antioxidant effects by directly neutralizing reactive oxygen species such as H_2O_2 or by serving as carriers for conventional antioxidants, thereby enhancing their bioavailability and stability. *Moringa oleifera* supports the host during parasitic infections by reducing oxidative stress and inflammation through its antioxidant compounds, while its direct antiparasitic activity is primarily attributed to tannins and saponins, which damage the parasites [28, 29]. Additionally, Mebendazole remains a first-choice drug for treatment of helminthiasis, as it induces only mild oxidative stress in the host [30].

This study has some limitations. First, it was conducted on a murine model, which may not fully replicate human trichinellosis, limiting direct clinical extrapolation. Second, the investigation focused on short-term outcomes without assessing long-term persistence of therapeutic effects or potential parasite recrudescence. Third, only one dosage and administration schedule of *Moringa* extract and nanoparticle formulations was tested, leaving dose–response relationships unexplored. Additionally, the study did not isolate or identify specific active phytochemicals within *Moringa* responsible for the observed effects, nor did it evaluate potential cytotoxicity or safety profiles of the nanoparticle formulations in non-infected models. Finally, the reliance on biochemical, histopathological, and parasitological parameters without molecular or immunological analyses restricts a deeper understanding of the mechanisms underlying the therapeutic benefits.

CONCLUSION

Overall, *Moringa oleifera* demonstrates considerable potential as an adjunctive therapy for trichinellosis, with nanoparticle formulation and combination strategies significantly enhancing its therapeutic efficacy.

RECOMMENDATION

Further studies are warranted to determine the optimal dose of *Moringa* extract and to elucidate the precise mechanisms underlying its therapeutic effects. Additionally, future research should focus on identifying the specific bioactive components released from *Moringa* and evaluating their potential cytotoxicity on normal cells.

Financial support and sponsorship: Nil.
Conflict of interest: Nil.

REFERENCES

1. Morsy T, Sallam TA, Hawam S (2022): Trichinosis (Trichinellosis) in Man And in Domestic and Wild Animals With Reference to Egypt: An Overview. Journal of the Egyptian Society of Parasitology, 52:431-42.
2. Sayed A, Hussein A, Arafa M *et al.* (2010): Epidemiological Study on Trichinellosis in Pigs and Man in Upper Egypt. Assiut Veterinary Medical Journal, 56:1-8.
3. Pozio E (2022): The impact of globalization and climate change on Trichinella spp. epidemiology. Food Waterborne Parasitol., 27:e00154.
4. Hassan Z, El-Sayed S, Zekry K *et al.* (2023): Impact of atorvastatin and mesenchymal stem cells combined with ivermectin on murine trichinellosis. Parasitol Res., 123:57.
5. Guo X, Luo W, Wu L *et al.* (2024): Natural Products from Herbal Medicine Self-Assemble into Advanced Bioactive Materials. Adv Sci (Weinh), 11:e2403388.
6. Pareek A, Pant M, Gupta M *et al.* (2023): Moringa oleifera: An Updated Comprehensive Review of Its Pharmacological Activities, Ethnomedicinal, Phytopharmaceutical Formulation, Clinical, Phytochemical, and Toxicological Aspects. Int J Mol Sci., 24(3):2098.
7. Fredericks J, Hill D, Zarlenga D *et al.* (2024): Inactivation of encysted muscle larvae of Trichinella spiralis in pigs using Mebendazole. Veterinary Parasitology, 327:110140.
8. Reitman S, Frankel S (1957): A colorimetric method for the determination of serum glutamic oxalacetic and glutamic pyruvic transaminases. Am J Clin Pathol., 28:56-63.
9. Patton J, Crouch S (1977): Spectrophotometric and kinetics investigation of the Berthelot reaction for the determination of ammonia. Analytical chemistry, 49:464-9.
10. Rosca E, Tudor R, Cornea A *et al.* (2021): Central Nervous System Involvement in Trichinellosis: A Systematic Review. Diagnostics (Basel), 11(6):945.
11. El-Sayed N, Fathy G (2019): Prophylactic and Therapeutic Treatments' Effect of Moringa Oleifera Methanol Extract on Cryptosporidium Infection in Immunosuppressed Mice. Anti-Infective Agents, 17:130-7.
12. Saad El-Din M, Gad El-Hak H, Ghobashy M *et al.* (2023): Parasitological and histopathological studies to the effect of aqueous extract of Moringa oleifera Lam. leaves combined with praziquantel therapy in modulating the liver and spleen damage induced by Schistosoma mansoni to male mice. Environ Sci Pollut Res Int., 30:15548-60.
13. Abdel-Latif M, El-Shahawi G, Aboelhadid S *et al.* (2018): Modulation of murine intestinal immunity by Moringa oleifera extract in experimental hymenolepiasis nana. J Helminthol., 92:142-53.
14. Dayanandan P, Cho W, Kang H *et al.* (2023): Emerging nano-scale delivery systems for the treatment of osteoporosis. Biomaterials Research, 27:68.
15. Adeyemi A, Ayoade A, Adejumo L *et al.* (2020): Influence of calcium nanoparticles (CaNPs) on nutritional qualities, radical scavenging attributes of Moringa oleifera and risk assessments on human health. Journal of Food Measurement and Characterization, 14:9.
16. Abd ES, Dyab A, Mahmoud A *et al.* (2024): Therapeutic effects of myrrh extract and myrrh-based silver nanoparticles on Trichinella spiralis-infected mice: parasitological, histopathological, and immunological (IFN-γ, IL-10, and MMP-9) investigations. Front Vet Sci., 11:1433964.
17. Codina A, Indelman P, Hinrichsen L *et al.* (2025): Significant Improvement in Bioavailability and Therapeutic Efficacy of Mebendazole Oral Nano-Systems Assessed in a Murine Model with Extreme Phenotypes of Susceptibility to Trichinella spiralis. Pharmaceutics, 17(8):1069.
18. Mira N, Henaish A, Moussa E *et al.* (2025): Improved Antiparasitic Effects of Mebendazole Using Chitosan and Zinc Oxide Nanocomposites for Drug Delivery in Trichinella spiralis Infected Mice During the Muscular Phase. Acta Tropica, 263:107565.
19. Elmelegy M, El M, Ghoneim N *et al.* (2019): Silver Nano Particles Improve the Therapeutic Effect of Mebendazole Treatment during the Muscular Phase of Experimental Trichinellosis, 6:9.
20. Fadil K, Mahmoud E, El-Ahl S *et al.* (2022): Investigation of the effect of the calcium channel blocker, verapamil, on the parasite burden, inflammatory response and angiogenesis in experimental Trichinella spiralis infection in mice. Food Waterborne Parasitol.. 26:e00144.
21. El-Wakil E, Shaker S, Aboushousha T *et al.* (2023): In vitro and in vivo anthelmintic and chemical studies of Cyperus rotundus L. extracts. BMC Complement Med Ther.. 23:15.
22. Nasreldin N, Swilam S, Abd-Elrahman S *et al.* (2022): Evaluation of Clinicopathological alterations in mice experimentally infected with Trichenella spiralis and the nematocidal effect of tannic acid and albendazole. New Valley Veterinary Journal, 2:16-27
23. Albogami B (2023): Ameliorative synergistic therapeutic effect of gallic acid and albendazole against Trichinella spiralis muscular phase infection and assessment of their effects on hepatic and cardiac tissues in male mice. Saudi J Biol Sci., 30:103763.
24. Henaish A, Mira N, Moussa E *et al.* (2025): Smart drug delivery system of nano-mebendazole medication, which depends on chitosan nanomolecule for murine trichinellosis treatment. Inorganic Chemistry Communications, 173:113843.
25. Derda M, Wandurska-Nowak E, Hadaś E (2004): Changes in the level of antioxidants in the blood from mice infected with Trichinella spiralis. Parasitology research, 93:207-10.
26. Pawłowska M, Mila-Kierzenkowska C, Szczegielniak J *et al.* (2023): Oxidative Stress in Parasitic Diseases-Reactive Oxygen Species as Mediators of Interactions between the Host and the Parasites. Antioxidants (Basel), 13(1):38.
27. Daré R, Lautenschlager S (2025): Nanoparticles with Antioxidant Activity. Antioxidants (Basel), 14:33.
28. Elghandour M, Maggiolino A, Vázquez-Mendoza P *et al.* (2023): Moringa oleifera as a Natural Alternative for the Control of Gastrointestinal Parasites in Equines: A Review. Plants (Basel), 12(9):1921.
29. Elmalawany A, Osman G, Mohamed A *et al.* (2024): Schistosomicidal Effects of Moringa oleifera Seed Oil Extract on Schistosoma mansoni-Infected Mice. Parasite Immunol., 46:e13070.
30. Locatelli C, Pedrosa R, De Bem A *et al.* (2004): A comparative study of albendazole and mebendazole-induced, time-dependent oxidative stress. Redox Rep., 9:89-95.